

Article

Roles of Silicon Content and Normalization Temperature on Cold Workability and Recrystallization of High-Grade Non-Oriented Silicon Steel

Yuan Lin ^{1,2}, Hongxia Wang ^{1,*}, Shijia Wang ¹, Wenkang Zhang ², Lixia Wang ², Zhiyuan Feng ³  and Yide Wang ^{1,2}

¹ College of Materials Science and Engineering, Taiyuan University of Technology, Taiyuan 030024, China; linyuan@tisco.com.cn (Y.L.); wangshijia1101@163.com (S.W.); wangyd@tisco.com.cn (Y.W.)

² Technical Center, Taiyuan Iron & Steel (Group) Co., Ltd., Taiyuan 030003, China; zhangwk@tisco.com.cn (W.Z.); wanglx1@tisco.com.cn (L.W.)

³ School of Chemical Engineering and Technology, Sun Yat-sen University, Zhuhai 519082, China; fengzhy25@mail.sysu.edu.cn

* Correspondence: wanghxia1217@163.com

Abstract: In order to decrease the difficulty of cold workability and study the recrystallization behavior of high-grade non-oriented silicon steel, Si content and normalization temperature were optimized simultaneously. The microstructure and texture of both hot-rolled sheet and normalized annealing sheet presented a gradient distribution. With the decrease in Si content from 3.02% to 2.54% and increase in normalization temperature from 850 °C to 920 °C, Goss texture ($\{110\}<001>$) intensity at surface layer and α -fiber ($\langle 110 \rangle // RD$) texture intensity were strengthened, and α -fiber texture gradually turned to α^* -fiber ($\{110\}<110>$) in the normalized annealing sheet. Recrystallization ratio and recrystallization grain size were increased both in the hot-rolled sheet and the normalized annealing sheet. The tensile strength and yield strength of normalized annealing sheet were reduced by 65 Mpa, which decreased the cold workability difficulty and improved cold rolling yield. The cold rolled microstructure had wider shear bands which nucleated earlier but recrystallized velocity was slower because of lower cold rolled energy storage during interval recrystallization annealing, resulting in a more heterogeneous grain size distribution in the final annealing sheet.

Keywords: high-grade non-oriented silicon steel; Si content; normalization temperature; workability; recrystallization behavior



Citation: Lin, Y.; Wang, H.; Wang, S.; Zhang, W.; Wang, L.; Feng, Z.; Wang, Y. Roles of Silicon Content and Normalization Temperature on Cold Workability and Recrystallization of High-Grade Non-Oriented Silicon Steel. *Crystals* **2022**, *12*, 593. <https://doi.org/10.3390/cryst12050593>

Academic Editors: Marina Polyakova and Marina Samodurova

Received: 30 March 2022

Accepted: 21 April 2022

Published: 23 April 2022

Publisher's Note: MDPI stays neutral with regard to jurisdictional claims in published maps and institutional affiliations.



Copyright: © 2022 by the authors. Licensee MDPI, Basel, Switzerland. This article is an open access article distributed under the terms and conditions of the Creative Commons Attribution (CC BY) license (<https://creativecommons.org/licenses/by/4.0/>).

1. Introduction

With the continuous upgrading of energy efficiency of high-efficiency compressor motors and electric motors, people have higher requirements for the magnetic properties of silicon steel [1,2]. Except for iron loss, there is a gradual increase in demanding magnetic induction properties. Conventional high-grade non-oriented silicon steel is mainly designed to reduce iron loss by increasing the content of Si and Al, especially by increasing the content of Si to meet the performance requirements of electric iron core motors [3,4]. However, the increase in Si content leads to a decrease in magnetic induction strength, and when the Si content increases to a certain degree, the cold working is difficult, and the yield is low [3,4]. The magnetic induction properties of high magnetic susceptibility non-oriented silicon steel are improved by increasing the normalization temperature, and at the same time, the iron loss is improved [5–8]. However, considering the difficulty of cold rolling, its Si content is lower than that of high-grade non-oriented silicon steel, and the iron loss cannot meet the needs of high efficiency motor applications. In this paper, the Si content and normalization temperature of high-grade non-oriented silicon steel were optimized. Designed and developed a high-grade non-oriented silicon steel product with low cost, good cold workability, and excellent iron loss.

2. Materials and Methods

The chemical composition of two different high-grade non-oriented silicon steel is shown in Table 1. The Si content of the 1# hot-rolled sheet is 3.02%, and the Si content of the 2# hot-rolled sheet is 2.54%. Using the same heating and hot rolling process, two different high-grade non-oriented silicon steels with different Si content were hot-rolled from 220 mm to 2.30 mm coil, and then normalized, cold-rolled, and annealed. The heating temperature of the cast slab was 1150 °C, the normalization temperature of sample 1 was 850 °C and sample 2 was 920 °C, and the normalization time of both samples was 3 min; finally, the cold-rolled sheets were annealed at 980 °C with a different interval of 3 s, 7 s, 15 s, 19 s, 23 s and 25 s, respectively, and the annealing atmosphere was 75% N₂ and 25% H₂. The detailed production process routes are shown in Figure 1.

Table 1. Chemical composition of two high grade non-oriented silicon steel.

Number	C	Si	Al	Mn	Ti	N	S	Note
1#	≤0.0045	3.02	0.32	0.17	≤0.0045	≤0.0045	≤0.0030	High silicon
2#	≤0.0045	2.54	0.35	0.15	≤0.0045	≤0.0045	≤0.0030	Low silicon

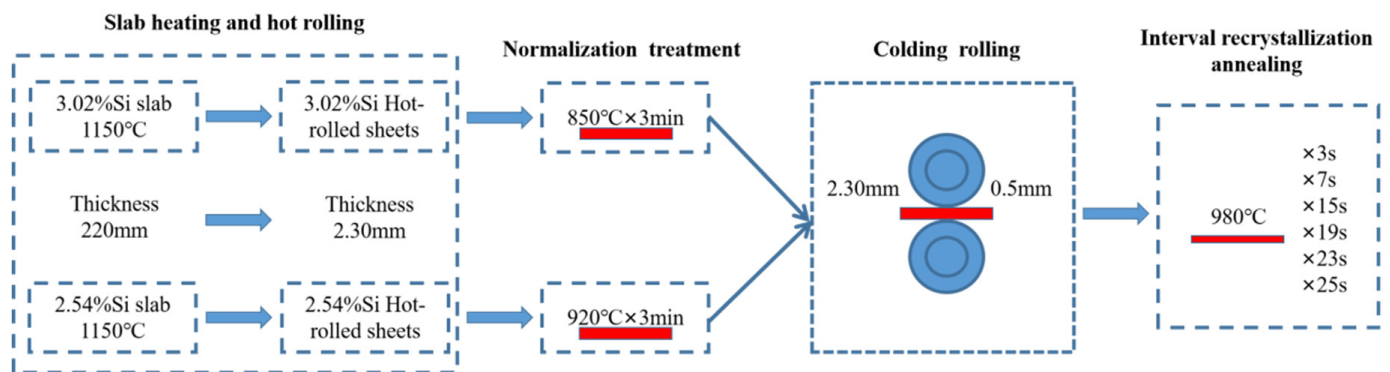


Figure 1. Schematic diagram of processing routes for the experimental steels.

After the test, microstructure, texture, and mechanical strength were observed and tested, respectively. The microstructure of the hot rolled sheet, normalized sheet, and interval annealing sheet were observed with the optical metallographic microscope (DMR, Leica, Germany), and the grain size was counted with image processing software. The etching solution was 4% HNO₃ in ethanol. The texture test was conducted on PANalytical's X-ray diffractometer, the sample size was 20 mm × 30 mm, the sampling surface was the RD-TD surface, and a cobalt target was used to obtain the ODF cross-sectional view according to the Bunge system. Finally, an electronic tensile tester (Zwick/Roell, Ulm, Germany) was used to conduct tensile tests of the two-component hot-rolled sheet specimens (sampling along the RD direction).

3. Results

3.1. Microstructure and Macro-Texture of High-Grade Non-Oriented Silicon Steel Initial Hot Rolled Sheet with Different Si Content

Figure 2 shows the microstructure and macro-texture of hot rolled sheets with 3.02% Si and 2.54% Si, respectively. The hot-rolled sheets with different Si content all presented a significant difference in microstructure and macro-texture along the thickness direction, which was consistent with the previous results on high-grade non-oriented silicon steel [1,2]. It can be found that the surface layer was mainly characterized by small recrystallized grains, while the center layer was elongated deformed grains, as shown in Figure 2a,c. Correspondingly, the macro-texture was dominated by Goss texture and randomly distributed α -fiber texture at surface layer with lower intensity, while very strong and relatively complete

α -fiber texture had a peak intensity at center layer $\{100\}\langle 110\rangle$, as shown in Figure 2e–h. The microstructure and macro-texture difference across thickness was related to deformation mode and temperature in hot rolling [3,4]. In contrast, when the Si content increased, the recrystallized ratio and grain size at the surface layer reduced, while Goss texture intensity weakened at the surface layer, but α -fiber texture at the center layer strengthened. However, it should be noted that the microstructure had a more inhomogeneous distribution when the Si content increased.

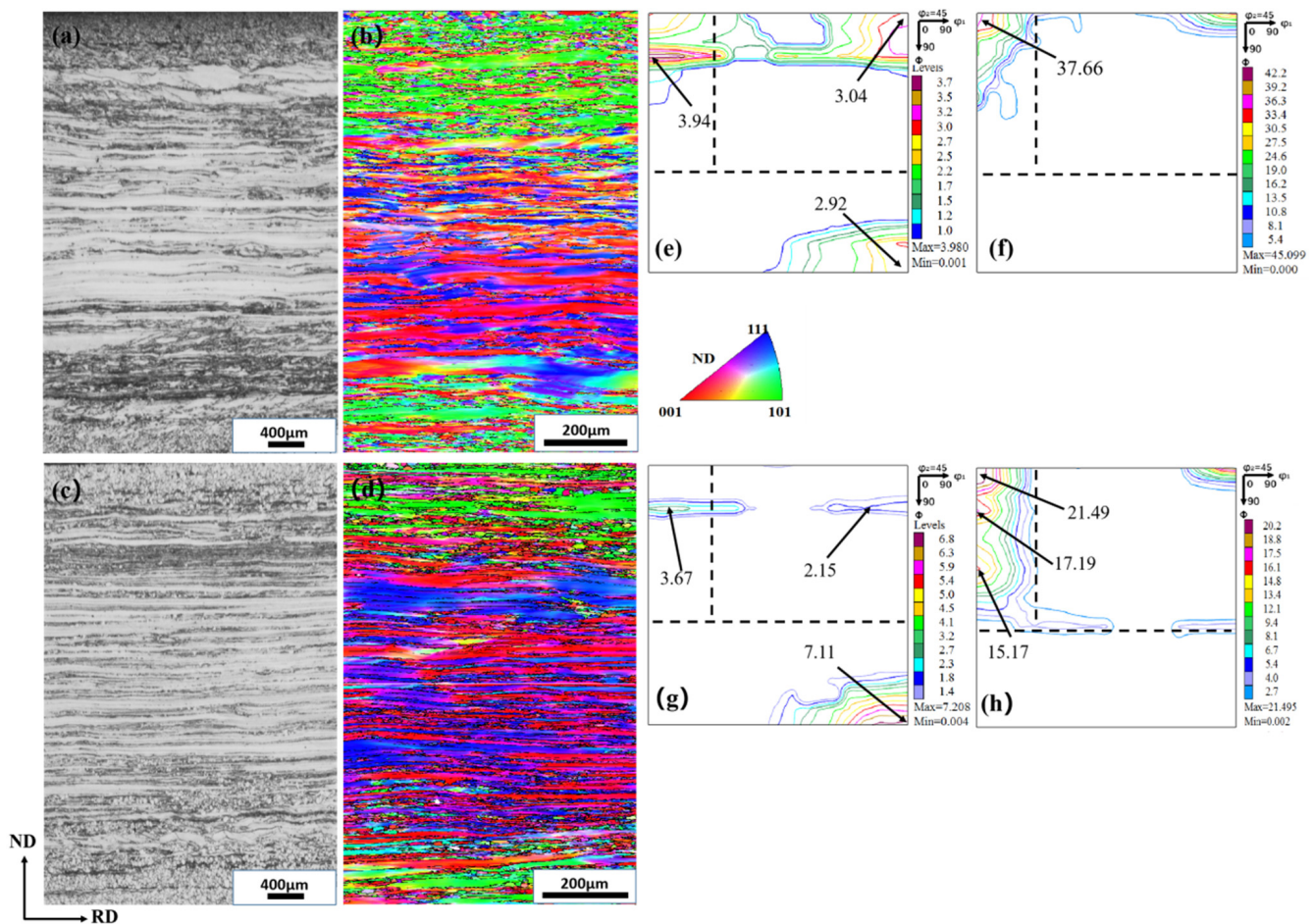


Figure 2. Microstructure (a,c), grain orientation image map (b,d) and macro-texture at surface region (e,g) and center region (f,h) of hot-rolled sheets with 3.02% Si content (upper) and 2.54% Si content (lower).

3.2. Microstructure and Macro-Texture and Mechanical Properties of High-Grade Non-Oriented Silicon Steel Normalized Sheets with Different Si Content at Different Normalization Temperature

Figures 3 and 4 show the microstructure, macro-texture, and grain size of normalized sheets with 3.02% Si and 2.54% Si, respectively. The normalized temperature was 850 °C and 920 °C, respectively. The microstructure of hot-rolled sheets with different Si content all completely recrystallized after normalization at different normalization temperatures, as shown in Figure 3a,c. In addition, the microstructure and macro-texture of normalized sheets were different between the surface layer and center layer which were consistent with hot rolled sheets. However, the texture intensity of normalized sheets decreased sharply, as shown in Figure 3e–h. According to Figure 3a,c, the average grain size at the surface layer was smaller than the center layer. Lower Si content with higher normalized temperature normalized sheet had a larger grain size and stronger $\{100\}\langle 110\rangle$ and Goss texture. Additionally, $\{113\}\langle 332\rangle$ was developed at the same time, as shown in Figure 3g. When Si content decreased and normalized temperature increased, α -fiber texture gradually

turned to α^* -fiber ($\{1\ 1\ h\}\langle 1/h\ 1\ 2\rangle$), and the intensity was strengthened. When the Si content decreased, tensile strength and yield strength of the normalization sheet were reduced by 65 MPa simultaneously, as shown in Figure 5. Per the results summarized in Figure 4, this method was able to decrease the workability of high-grade non-oriented silicon steel.

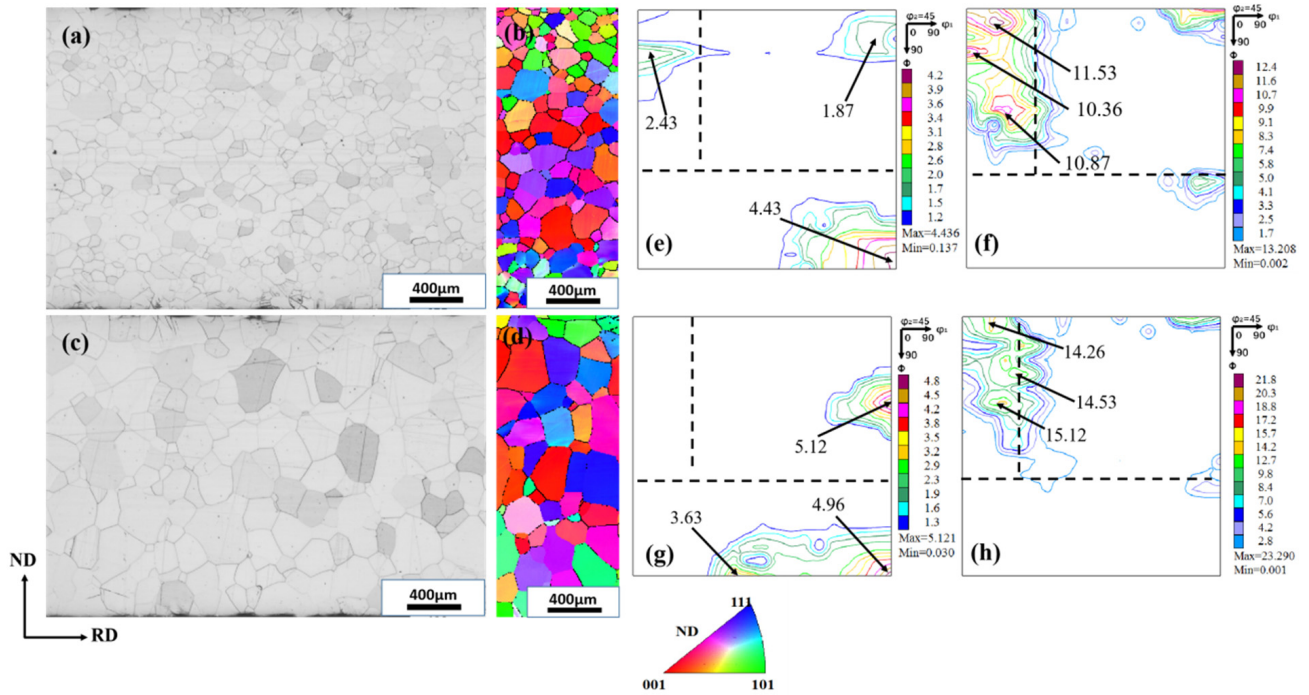


Figure 3. Microstructure (a,c), grain orientation image map (b,d), and macro-texture at surface region (e,g) and center region (f,h) of normalized sheets (corresponding normalization temperature were 850 °C and 920 °C, respectively) with 3.02% Si content (upper) and 2.54% Si content (lower).

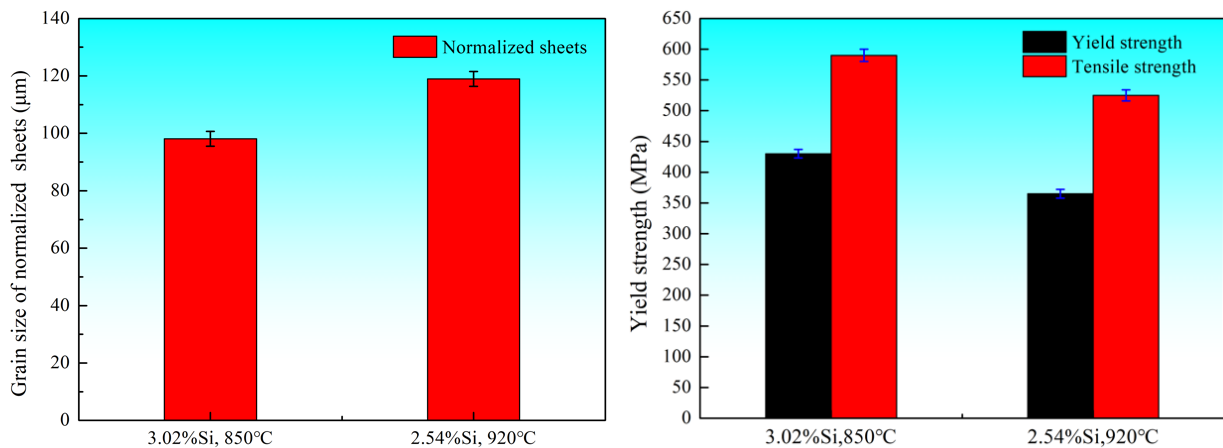


Figure 4. Grain size and mechanical properties of normalized sheets with different Si content and normalization temperature. The detailed statistical information is in Tables S1 and S2.

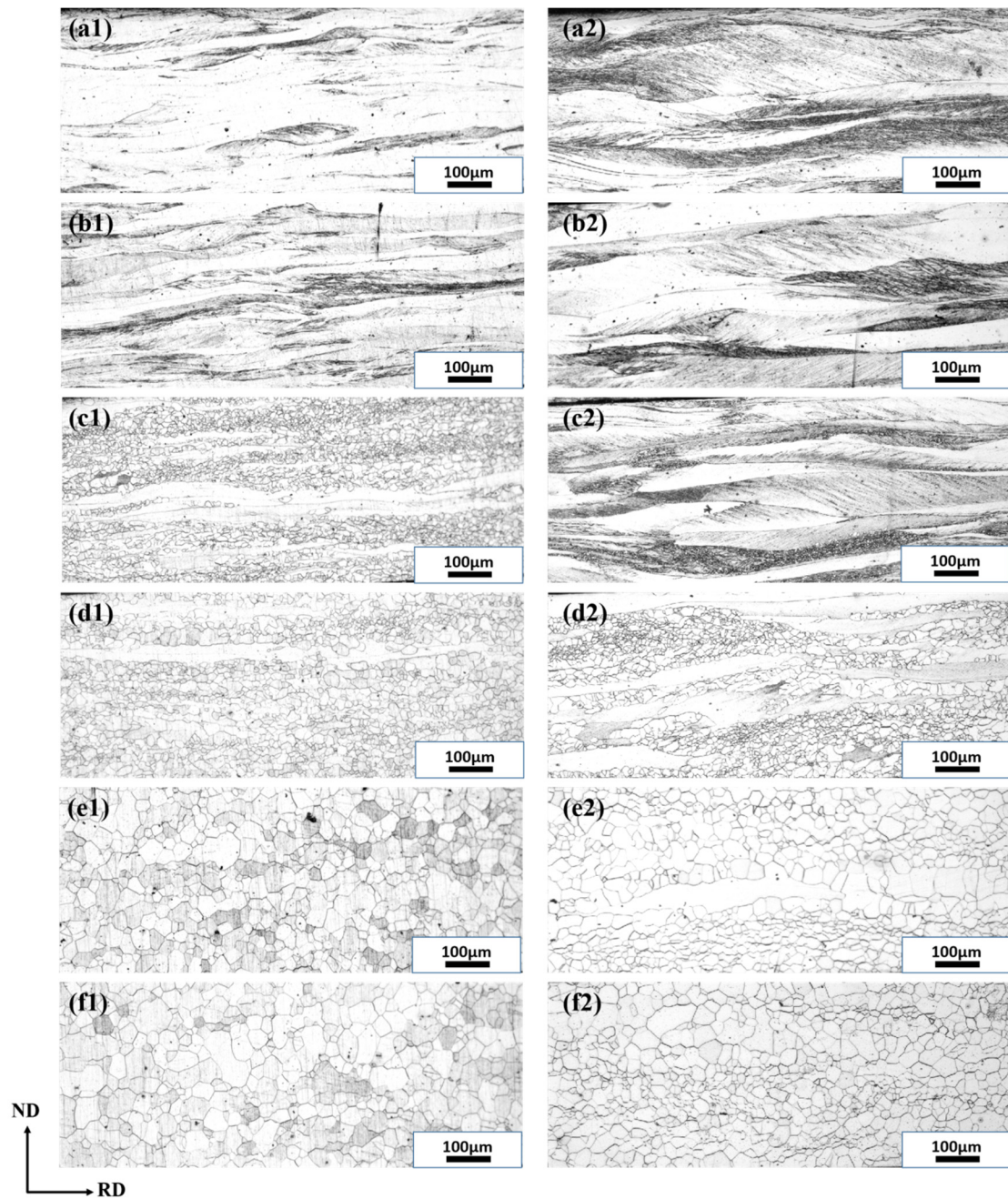


Figure 5. Recrystallization microstructure evolution of the cold rolled sheets of 3.02% Si content (**left**) and 2.54% Si content (**right**) for different intervals: (**a1,a2**) 3 s; (**b1,b2**) 7 s; (**c1,c2**) 15 s; (**d1,d2**) 19 s; (**e1,e2**) 23 s; (**f1,f2**) 25 s.

4. Discussion

4.1. Role of Silicon Content on Hot-Rolled Microstructure and Texture of High-Grade Non-Oriented Silicon Steel

Silicon is one of the most important elements of non-oriented silicon steel, which can effectively reduce iron loss [5–8]. However, the increase in Si content leads to an increase in lattice distortion and ordered phase, which, in turn, hinders the dislocation motion [9–12]. Therefore, when the Si content increases, the dynamic recrystallization of high-grade non-oriented silicon steel is hindered, the recrystallization ratio of the surface layer of the hot-rolled sheet decreases, the recrystallization size decreases, and the Gaussian texture strength also decreases, as shown in Figure 3a,c,e,g. Additionally, with the increase

in Si content, the hot deformation activation energy of the hot-rolled sheet increases [13,14], and, under surface stress, the α -fiber texture strength of the central layer of the hot-rolled sheet increases [15,16], as shown in Figure 3f,h.

4.2. Role of Silicon Content and Normalization Temperature on Recrystallization Kinetics of High-Grade Non-Oriented Silicon Steel

Previous studies have reported the effects of typical alloying elements and normalization temperature on crystallization kinetics and texture [17–20], but the combined effects of these two factors have not been clearly elucidated. To understand the combined effect of Si content and normalization temperature on the recrystallization behavior, the recrystallization process was tracked by intermittent annealing at 980 °C on 3.02% Si and 2.54% Si cold plates. The microstructures at different annealing times are shown in Figure 5. After annealing for 3 s, recrystallization occurred in both cold-rolled sheets, and the initial nucleation point was on the shear band. The number of recrystallized grains in the 2.54% Si (normalization at 920 °C) cold-rolled sheet was larger. After annealing for 7 s, the recrystallized grains of the 3.02% Si (normalization at 850 °C) cold-rolled sheet increased, and the uniform distribution of nucleation points was not limited to the shear band. However, the nucleation point and recrystallization ratio of the 2.54% Si cold plate are basically unchanged, as shown in Figure 5(a2,b2). After annealing for 15 s, the recrystallization ratio of the 3.02% Si cold plate increased dramatically and far exceeded that of the 2.54% Si cold plate, but the grains in the center layer of the 2.54% Si cold-rolled plate were still in a state of slight tensile deformation, as shown in Figure 5(c1,c2). Finally, the 3.02% Si and 2.54% Si cold plates with different normalization temperatures undergo complete recrystallization at 23 s and 25 s, respectively, as shown in Figure 5(e1,f2).

As presented in Figure 6, compared with the finished annealed sheet of high-grade non-oriented 3.02% Si steel with a normalization temperature of 850 °C, the annealed 2.54% Si sheet with a normalization temperature of 920 °C had a stronger λ -fiber ($\langle 001 \rangle // \text{ND}$) texture and weaker γ -fiber ($\langle 111 \rangle // \text{ND}$) texture. However, the latter cold-rolled sheet had low and uneven recrystallization energy storage and early nucleation during intermittent annealing. However, the recrystallization rate was slow, and the grain size of the finished plate was extremely uneven.

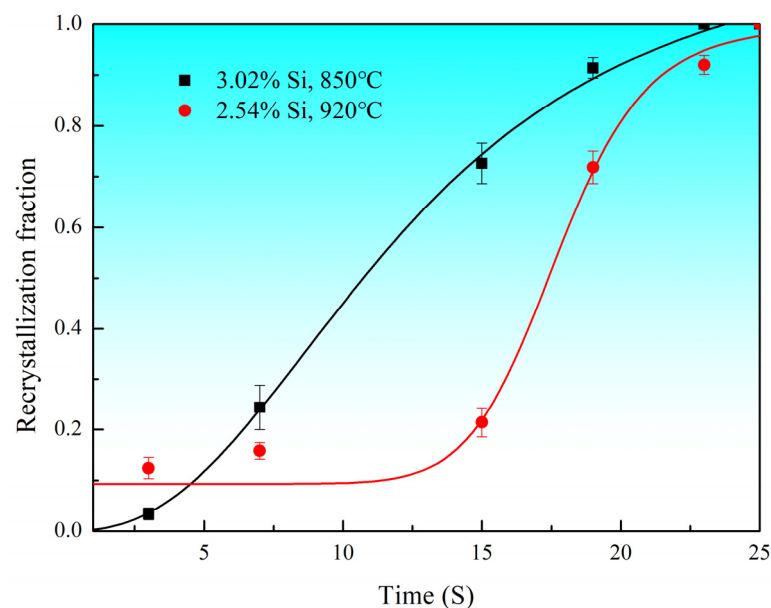


Figure 6. Comparison of recrystallization fraction of the cold-rolled sheets of different Si content with different normalization temperature. The detailed statistical information is in Tables S3 and S4.

When the Si content decreased from 3.02% to 2.54% and the normalization temperature increased from 850 °C to 920 °C, the grain size of the normalized annealing sheet became larger, and the time required for complete recrystallization of the cold plate increased slightly. However, because of the high annealing temperature of cold-rolled sheets, the annealed average grain size of high-silicon and low-silicon products was basically the same. Therefore, both the iron loss and the magnetic polarization of the annealed sheet were improved. The iron loss P1.5/50 was reduced from 2.73 W/kg to 2.62 W/kg, and the magnetic polarization J5000 was increased from 1.681 to 1.704 T.

5. Conclusions

- (1) Si hindered recrystallization and increased deformation resistance. When Si content decreased, recrystallization ratio, recrystallized grain size and Goss texture intensity at the surface layer of high-grade non-oriented silicon steel hot rolled sheet increased, but α -fiber texture intensity at the center layer reduced.
- (2) When the Si content decreased, tensile strength and yield strength of the normalized sheet were reduced by 65 MPa simultaneously; this method was able to decrease the cold rolling workability evidently of high-grade non-oriented silicon steel.
- (3) Lower Si content and higher normalization temperature cold-rolled sheet had more shear bands that nucleated earlier but the process of recrystallization was slower, resulting in a more heterogeneous grain size distribution in the final annealing sheet.

Supplementary Materials: The following supporting information can be downloaded at: <https://www.mdpi.com/article/10.3390/cryst12050593/s1>, Table S1: Grain size of normalized sheets with different Si content and normalization temperature; Table S2: Mechanical properties of normalized sheets with different Si content and normalization temperature; Table S3: Recrystallization fraction of the cold rolled sheet of 3.02% Si and normalized at 850 °C; Table S4: Recrystallization fraction of the cold rolled sheet of 2.54% Si and normalized at 920 °C.

Author Contributions: Conceptualization, Y.L., H.W. and S.W.; methodology, Y.L., H.W., S.W., W.Z. and L.W.; formal analysis, Y.L., H.W. and S.W.; investigation, Y.L., H.W. and S.W.; data curation, Y.L., H.W. and S.W.; writing—original draft preparation, Y.L.; writing—review and editing, H.W. and Z.F.; supervision, H.W.; project administration, H.W. and Y.W. All authors have read and agreed to the published version of the manuscript.

Funding: This work was supported by the Science and Technology Major Project of Shanxi Province (20191102004).

Institutional Review Board Statement: Not applicable.

Informed Consent Statement: Not applicable.

Data Availability Statement: Not applicable.

Conflicts of Interest: The authors declare no conflict of interest.

References

1. Petrun, M.; Steentjes, S. Iron-loss and magnetization dynamics in non-oriented electrical steel: 1-D excitations up to high frequencies. *IEEE Access* **2020**, *8*, 4568–4593. [[CrossRef](#)]
2. Barros, J.; Ros-Yanez, T.; Vandenbossche, L.; Dupré, L.; Melkebeek, J.; Houbaert, Y. The effect of Si and Al concentration gradients on the mechanical and magnetic properties of electrical steel. *J. Magn. Magn. Mater.* **2005**, *290*, 1457–1460. [[CrossRef](#)]
3. Ban, G.; Nemeth, S.; Arato, P. Composition effects on core loss of Fe-Si-Al electrical steels. *IEEE Trans. Magn.* **1987**, *23*, 3227–3229. [[CrossRef](#)]
4. Ros-Yáñez, T.; Ruiz, D.; Barros, J.; Houbaert, Y. Advances in the production of high-silicon electrical steel by thermomechanical processing and by immersion and diffusion annealing. *J. Alloys Compd.* **2004**, *369*, 125–130. [[CrossRef](#)]
5. Moseley, D.; Hu, Y.; Randle, V.; Irons, T. Role of silicon content and final annealing temperature on microtexture and microstructure development in non-oriented silicon steel. *Mater. Sci. Eng. A* **2005**, *392*, 282–291. [[CrossRef](#)]
6. An, L.Z.; Wang, Y.; Song, H.Y.; Wang, G.-D.; Liu, H.-T. Improving magnetic properties of non-oriented electrical steels by controlling grain size prior to cold rolling. *J. Magn. Magn. Mater.* **2019**, *491*, 165636. [[CrossRef](#)]

7. Park, J.T.; Szipunar, J.A. Effect of initial grain size on texture evolution and magnetic properties in nonoriented electrical steels. *J. Magn. Magn. Mater.* **2009**, *321*, 1928–1932. [[CrossRef](#)]
8. Shiozaki, M.; Kurosaki, Y. The effects of grain size on the magnetic properties of non-oriented electrical steel sheets. *J. Mater. Eng.* **1989**, *11*, 37–43. [[CrossRef](#)]
9. Li, Z.H.; Xie, S.K.; Wang, G.D.; Liu, H.-T. Dependence of recrystallization behavior and magnetic properties on grain size prior to cold rolling in high silicon non-oriented electrical steel. *J. Alloys Compd.* **2021**, *888*, 161576. [[CrossRef](#)]
10. Liang, Y.F.; Ye, F.; Lin, J.P.; Wang, Y.L.; Chen, G.L. Effect of annealing temperature on magnetic properties of cold rolled high silicon steel thin sheet. *J. Alloys Compd.* **2010**, *491*, 268–270. [[CrossRef](#)]
11. Li, Z.; Xie, S.; Wang, G.; Liu, H.-T. Ultrathin-gauge high silicon non-oriented electrical steel with high permeability and low core loss fabricated by optimized two-stage cold rolling method. *Mater. Charact.* **2022**, *183*, 111593. [[CrossRef](#)]
12. Cai, G.; Li, C.; Cai, B.; Wang, Q. An investigation on the role of texture evolution and ordered phase transition in soft magnetic properties of Fe–6.5 wt% Si electrical steel. *J. Magn. Magn. Mater.* **2017**, *430*, 70–77. [[CrossRef](#)]
13. Mehdi, M.; He, Y.; Hilinski, E.J.; Kestens, L.A.; Edrissy, A. The evolution of cube ($\{001\}<100>$) texture in non-oriented electrical steel. *Acta Mater.* **2020**, *185*, 540–554.
14. Sidor, Y.; Kovac, F. Microstructural aspects of grain growth kinetics in non-oriented electrical steels. *Mater. Charact.* **2005**, *55*, 1–11. [[CrossRef](#)]
15. Fang, F.; Xu, Y.B.; Zhang, Y.X.; Wang, Y.; Lu, X.; Misra, R.; Wang, G.-D. Evolution of recrystallization microstructure and texture during rapid annealing in strip-cast non-oriented electrical steels. *J. Magn. Magn. Mater.* **2015**, *381*, 433–439. [[CrossRef](#)]
16. Zu, G.; Xu, Y.; Luo, L.; Han, Y.; Sun, S.; Miao, R.; Zhu, W.; Gao, L.; Ran, X. Effect of rolling temperature on the recrystallization behavior of 4.5 wt.% Si non-oriented electrical steel. *J. Mater. Res. Technol.* **2022**, *17*, 365–373. [[CrossRef](#)]
17. Džubinský, M.; Sidor, Y.; Kováč, F. Kinetics of columnar abnormal grain growth in low-Si non-oriented electrical steel. *Mater. Sci. Eng. A* **2004**, *385*, 449–454. [[CrossRef](#)]
18. Jiao, H.T.; Xu, Y.B.; Zhao, L.Z.; Misra, R.; Tang, Y.; Zhao, M.; Liu, D.; Hu, Y.; Shen, M. Microstructural evolution and magnetic properties in strip cast non-oriented silicon steel produced by warm rolling. *Mater. Charact.* **2019**, *156*, 109876. [[CrossRef](#)]
19. Da Costa Paolinelli, S.; da Cunha, M.A.; Cota, A.B. The influence of shear bands on final structure and magnetic properties of 3% Si non-oriented silicon steel. *J. Magn. Magn. Mater.* **2008**, *320*, e641–e644. [[CrossRef](#)]
20. De Dafe, S.S.F.; da Costa Paolinelli, S.; Cota, A.B. Influence of thermomechanical processing on shear bands formation and magnetic properties of a 3% Si non-oriented electrical steel. *J. Magn. Magn. Mater.* **2011**, *323*, 3234–3238. [[CrossRef](#)]